

Anomalous valley Hall effect in two-dimensionalvalleytronic materials

Hongxin Chen(陈洪欣), Xiaobo Yuan(原晓波), and Junfeng Ren(任俊峰)1

Citation: Chin. Phys. B, 2024, 33 (**4**): 047304. DOI: 10.1088/1674-1056/ad1c59
Journal homepage: http://cpb.iphy.ac.cn; http://iopscience.iop.org/cpb

What follows is a list of articles you may be interested in

Anomalous valley Hall effect in two-dimensional valleytronic materials

Hongxin Chen(陈洪欣), Xiaobo Yuan(原晓波), and Junfeng Ren(任俊峰)
Chin. Phys. B, 2024, 33 (**4**): 047302. DOI: 10.1088/1674-1056/ad1c59

Recent progress on valley polarization and valley-polarized topological states in two-dimensional materials

Fei Wang(王斐), Yaling Zhang(张亚玲), Wenjia Yang(杨文佳), Huisheng Zhang(张会生), and Xiaohong Xu(许小红)
Chin. Phys. B, 2024, 33 (**1**): 017306. DOI: 10.1088/1674-1056/ad0713

Perspectives of spin-valley locking devices

Lingling Tao(陶玲玲)
Chin. Phys. B, 2023, 32 (**10**): 107306. DOI: 10.1088/1674-1056/acc809

Single-layer intrinsic 2H-phase LuX_2 (X = Cl, Br, I) with large valley polarization and anomalous valley Hall effect

Chun-Sheng Hu(胡春生), Yun-Jing Wu(仵允京), Yuan-Shuo Liu(刘元硕), Shuai Fu(傅帅),Xiao-Ning Cui(崔晓宁), Yi-Hao Wang(王易昊), and Chang-Wen Zhang(张昌文)
Chin. Phys. B, 2023, 32 (**3**): 037306. DOI: 10.1088/1674-1056/ac89d6

Spin- and valley-polarized Goos-Hänchen-like shift in ferromagnetic mass graphene junction with circularly polarized light

Mei-Rong Liu(刘美荣), Zheng-Fang Liu(刘正方), Ruo-Long Zhang(张若龙), Xian-Bo Xiao(肖贤波), and Qing-Ping Wu(伍清萍)
Chin. Phys. B, 2023, 32 (**3**): 037301. DOI: 10.1088/1674-1056/ac89e2

TOPICAL REVIEW — Valleytronics

Anomalous valley Hall effect in two-dimensional valleytronic materials

Hongxin Chen(陈洪欣)[1], Xiaobo Yuan(原晓波)[1], and Junfeng Ren(任俊峰)[1,2,†]

[1] *School of Physics and Electronics, Shandong Normal University, Jinan* 250358, *China*

[2] *Shandong Provincial Engineering and Technical Center of Light Manipulations & Institute of Materials and Clean Energy, Shandong Normal University, Jinan* 250358, *China*

(Received 7 October 2023; revised manuscript received 21 December 2023; accepted manuscript online 9 January 2024)

The anomalous valley Hall effect (AVHE) can be used to explore and utilize valley degrees of freedom in materials, which has potential applications in fields such as information storage, quantum computing and optoelectronics. AVHE exists in two-dimensional (2D) materials possessing valley polarization (VP), and such 2D materials usually belong to the hexagonal honeycomb lattice. Therefore, it is necessary to achieve valleytronic materials with VP that are more readily to be synthesized and applicated experimentally. In this topical review, we introduce recent developments on realizing VP as well as AVHE through different methods, i.e., doping transition metal atoms, building ferrovalley heterostructures and searching for ferrovalley materials. Moreover, 2D ferrovalley systems under external modulation are also discussed. 2D valleytronic materials with AVHE demonstrate excellent performance and potential applications, which offer the possibility of realizing novel low-energy-consuming devices, facilitating further development of device technology, realizing miniaturization and enhancing functionality of them.

Keywords: anomalous valley Hall effect, valley polarization, valleytronics, two-dimensional materials

PACS: 73.20.Hb, 73.22.–f, 75.50.Pp, 75.76.+j **DOI:** 10.1088/1674-1056/ad1c59

1. Introduction

In recent years, two-dimensional (2D) materials have attracted intensive attention due to their superior properties compared to three-dimensional materials, such as good ductility and quantum confinement effect.[1–6] One of the exciting news is that researchers have discovered valley in 2D hexagonal honeycomb lattice materials. Valley, the energy extrema in the conduction and valence bands at the momentum space, is a new degree of freedom for performing information encoding and storage analogous to charge and spin.[7–11] The studies of valley degree of freedom have now become a new research field, valleytronics, in condensed matter physics.[12] Transition metal dichalcogenides (TMDs) are a class representative of 2D valleytronic materials, which have been widely studied due to the broken of space-inversion symmetry leading to the presence of degeneracy but inequivalent K valleys discretely in momentum space.[13–17] The spin–valley coupling can be observed in H-phase TMDs owing to the protection of time-reversal symmetry.[18–20] The Berry curvature of these materials is equal in size and opposite in direction at the K and K' points, therefore, the valley Hall effect (VHE) characterized by the valley Chern number C_v can be realized.[11,21–24] At present, many 2D valleytronic materials with VHE have been theoretically predicted and experimentally synthesized, such as monolayer MoS_2, Janus monolayers TiXY ($X \neq Y$, X/Y = Cl, Br, I), monolayer MN_2X_2 (M = Mo, W; X = F, H), monolayer $MoSi_2N_4$ and monolayer H-ZrX_2 (X = Cl, Br, I).[18,24–29] These lay the material foundation for designing promising valleytronic devices.

However, 2D materials with VHE possess degenerate valleys, which makes it challenging to distinguish and manipulate valley degrees of freedom and limits the application in direct information storage.[12,30,31] This is attributed to the fact that electrons can scatter freely between different valleys, resulting in uncontrolled energy and momentum of the electrons, making it difficult to achieve precise electronic manipulation. Therefore, 2D materials with non-degenerate valleys, i.e., with valley polarization (VP), are more suitable for specific applications, such as quantum computing and novel electronic devices, due to the fact that they allow a more precise control of the state of the electrons.[32–34] That is why it is necessary to break the degeneracy of valley to achieve VP. The question is how the degeneracy of valleys can be lifted. Obviously, many researchers have made attempts and obtained many useful methods as of now. For example, the realization of VP through circularly polarized optical pumping and the optical Stark effect is limited by the extremely short carrier lifetime, and researchers are still striving for breakthroughs in this direction.[35–37] A VP of 0.1 meV–0.2 meV requires an external magnetic field of 1 T to realize, which is clearly an un-

†Corresponding author. E-mail: renjf@sdnu.edu.cn

© 2024 Chinese Physical Society and IOP Publishing Ltd

satisfactory result.[38–41] However, this has led researchers to ponder whether they could introduce magnetism into the material to obtain a more satisfactory phenomenon. The methods such as the magnetic atoms doping, coupling with magnetic proximity, and searching for materials with intrinsic magnetic moments emerge one by one along with the development of valleytronics, which in turn causes a research boom.[31,42–55] When a valley is passed through by the Fermi level, which can be modulated by electron doping or by applying a gate voltage, the carriers at the valley acquire anomalous velocities and converge to one boundary of the material in the presence of a transverse electric field, generating in a net Hall current, thus realizing the anomalous valley Hall effect (AVHE) in materials with VP.[31]

In this review, we present the development of the introduction of magnetism to the system to realize VP as well as the AVHE, mainly based on our own work. By using monolayer WSSe and WTe_2 as examples, we introduce the relevant research progress in realizing VP and AVHE through doping or adsorbing transition metal atoms in Section 2. Section 3 shows that VP and AVHE can be realized by using the magnetic proximity effect and case studies of three ferrovalley heterostructure material systems are provided. In Section 4, the limitations of the previous two sections are discussed, and several ferrovalley materials with spontaneous VP as well as the AVHE and the external field modulation are introduced. We provide an overview of the main findings of the previous sections and future directions of valleytronics in Section 5.

2. Doping/adsorption of transition metals to obtain VP and AVHE

The spin degeneracy of the reported 2D valleytronic materials with VHE is lifted due to the spin orbital coupling (SOC) and their K and K' valleys are protected by time-reversal symmetry to exhibit energy degeneracy.[16,27,28] It is possible to obtain VP and AVHE by introducing magnetism that breaks the time-reversal symmetry of 2D valleytronic materials with VHE. The equilibrium VP can be obtained in 2D dilute magnetic semiconductor Mn-doped MoS_2 after considering SOC.[42,56] Furthermore, the emergence of VP and AVHE are predicted both in the works of monolayer MoS_2 adsorbed with transition metal atoms and Janus monolayer MoSSe doped with magnetic atoms.[43,44] These theoretical results prove that the introduction of magnetism by doping or adsorption of transition metal atoms can lift the degeneracy of energy for the K and K' valleys in the formed new valleytronic system, resulting in VP, so AVHE can be obtained. Moreover, it is challenging to obtain a large VP, and a large VP is of great value for the potential practical applications of AVHE, so it is necessary to enrich the 2D valleytronic material systems that are doped with transition metal atoms to achieve VP.

2.1. Doping/adsorption of transition metal in Janus WSSe

The 2D Janus MXY (M = Mo, W; X,Y = S, Se, Te; $X \neq Y$) with C_{3v} symmetry results in a series of exotic properties due to its symmetry-broken structure, such as strong Rashba effect, significant piezoelectric effect, and good catalytic properties, which has inspired a tremendous interest in the investigation of MXY materials.[57,58] Here, Zhao *et al.* focused their attention on the valleytronic properties of monolayer WSSe.[59] Figure 1(a) shows the top and side views of the monolayer WSSe after complete relaxation, where the red balls represent the doping/adsorption sites. The pristine monolayer WSSe is protected by time-reversal symmetry and the space-inversion symmetry is broken, then the energies of the K and K' valleys are degenerate and the signs of the spin and Berry curvature at both valleys are opposite when considering SOC in Fig. 1(b). This means that when a transverse external electric field is applied to monolayer WSSe, injection of holes into the system results in different spin valley Hall currents being observed at different boundaries of the material due to the carriers acquiring opposite velocities at the K and K' valleys (Fig. 1(g)), i.e., the VHE is realized.

For providing practical methods to explore valley degrees of freedom of monolayer WSSe, doping/adsorption of transition metals is considered to realize VP and AVHE. For doping transition metals, the difference in hybridization between the impurity energy levels and the highest valence band of the monolayer WSSe leads to the fact that doping of V atom can induce a large VP of 58 meV in Fig. 1(c), whereas doping of Cr (Fig. 1(d)), Mn, Fe, and Co atoms can only induce a negligible VP. For the adsorption of transition metals, take the adsorption of Cr atoms as an example, since the interaction between Cr atoms and S atoms is stronger than that between Cr atoms and Se atoms during the adsorption process, the adsorption of Cr atoms on the surface of Se generates a large VP of 62 meV (Fig. 1(e)), whereas the VP is suppressed when adsorbed on the surface of S (Fig. 1(f)). The VP can be obtained in monolayer WSSe by doping/adsorption of transition metals due to the time-reversal symmetry is broken by the introduced magnetism. Obviously, for systems possessing a VP, carriers on only one K valley gain anomalous velocities under a transverse external electric field (Fig. 1(h)), resulting in the formation of a valley Hall current on one boundary of the material, which is AVHE that can be used in spin–valley devices. Inducing and controlling VP in 2D materials is fraught with important implications and challenges, and the results of this work provide some theoretical basis for this.

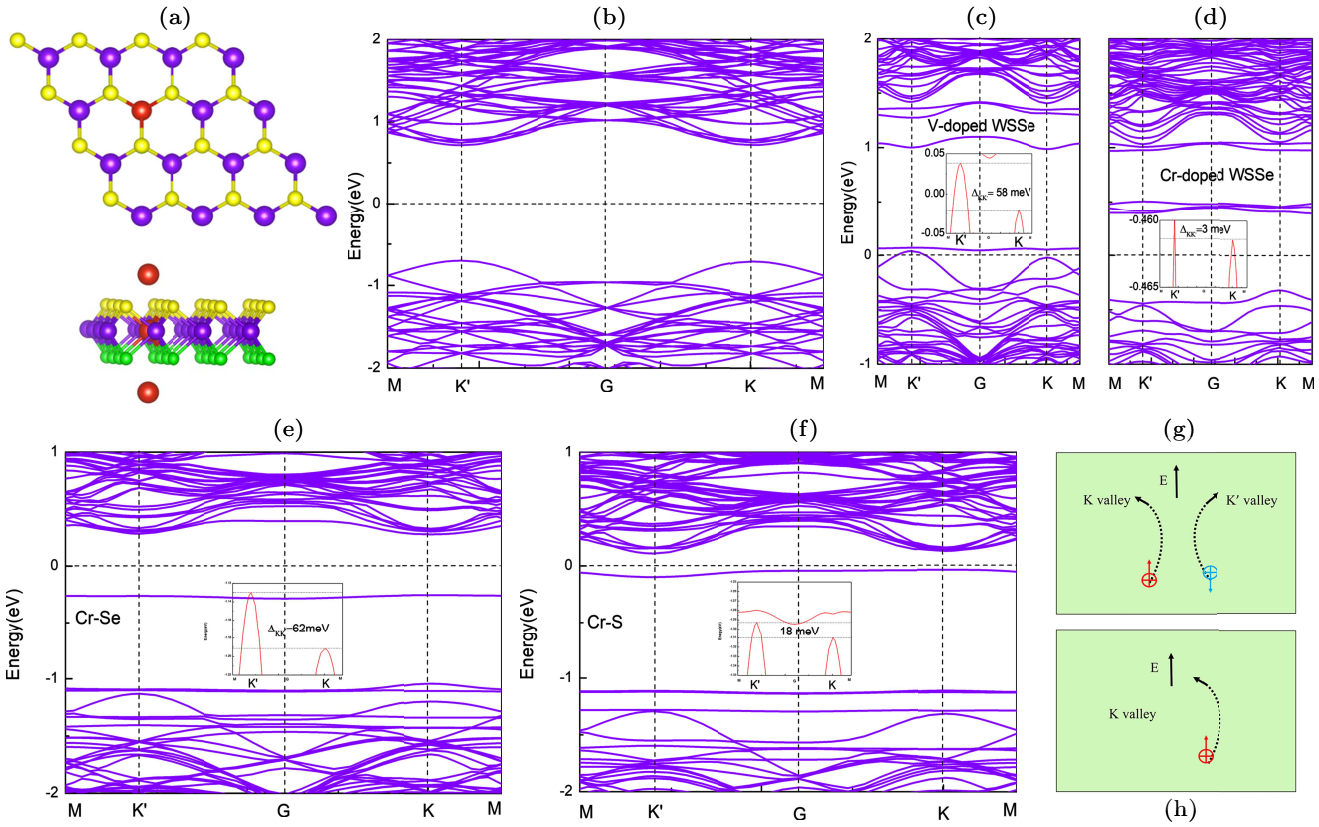


Fig. 1. (a) The top and side views of the monolayer WSSe, where the yellow, green, purple, and red balls represent S, Se, W atoms and the doping/adsorption sites, respectively. (b) The band structure of pristine monolayer WSSe with SOC. (c) and (d) The band structure of the considered SOC for monolayer WSSe doped with V and Cr, respectively. (e) and (f) The band structure of the system with SOC when Cr is adsorbed on the top of the Se and S surfaces, respectively. (g) Diagram of the VHE. (h) Diagram of the monolayer AVHE in WSSe with Cr adsorbed on the top of the Se-surface.[59]

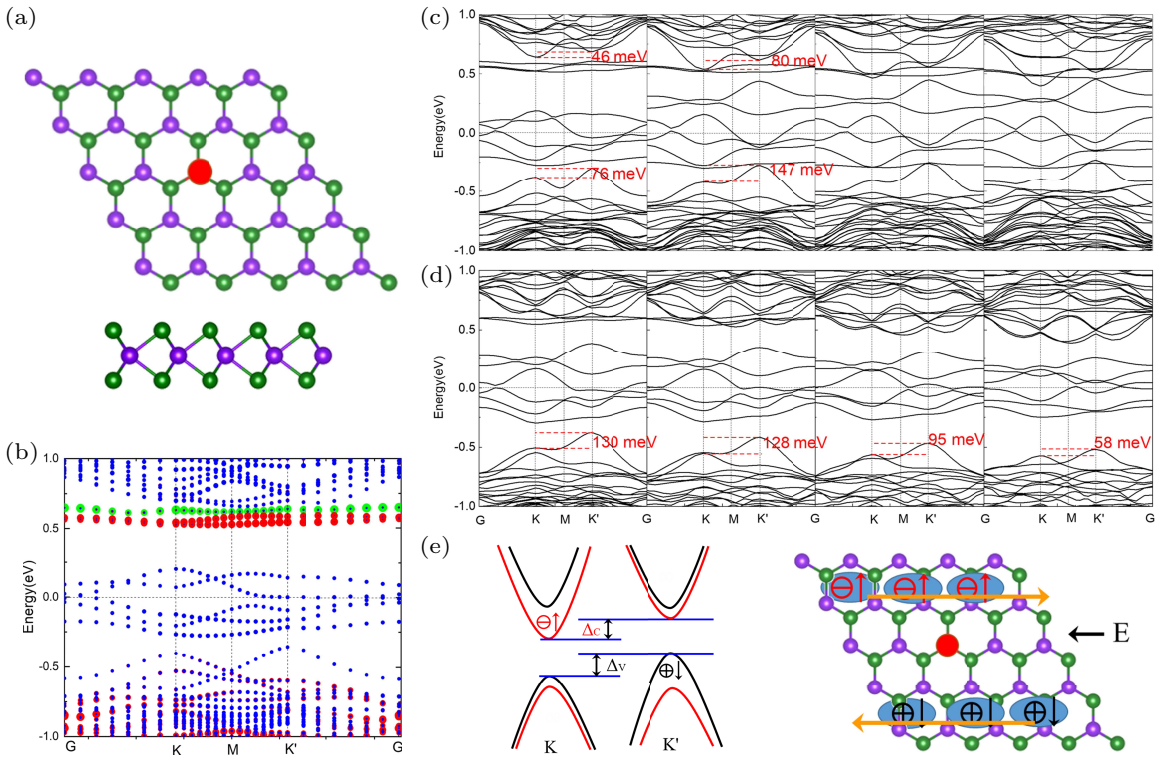


Fig. 2. (a) The top and side views of the monolayer WTe_2, where the purple, green, and red balls represent W, Te, and the doping sites, respectively. (b) The band structure of Co-doped monolayer WTe_2 with SOC. (c) and (d) The band structure of the considered SOC for Co-doped monolayer WTe_2 under tension strain of 1%–4% and compression strain from -1% to -4%, respectively. (e) Diagram of band structure and spin valley Hall effect under external electric field with both holes and electrons as carriers.[60]

2.2. Transition-metal-doped WTe_2 and strain modulation

It remains exciting to find suitable 2D materials and utilize appropriate modulation methods to obtain VP to drive AVHE applications. Zhao *et al.* further investigated the effect of strain on the valleytronic properties of monolayer WTe_2 systems doped with transition metal atoms based on previous work.[60] The negative formation energy proves the stability of monolayer WTe_2 (Fig. 2(a)) doped with Sc, Ti, V, Cr, Mn, Fe, Co, and Ni atoms, respectively. It is found that doping of Co atom produced the most satisfactory phenomena, because the Co atom doping in WTe_2 introduces magnetism and the impurity energy level in the system does not affect the integrity of the energy valley of WTe_2. The valleys of the system remain complete and the K and K' valleys are not degenerate under the combined effect of magnetism introduced by Co atom doping and SOC, which achieves a VP of 46 meV (Fig. 2(b)) sufficient for the AVHE at room temperature. In addition, the VP can be enhanced by applying a biaxial strain (Figs. 2(c) and 2(d)) to the system, where the maximum VP in the conduction and valence bands are 80 meV and 147 meV, respectively. The VP can exist in both the conduction and valence bands in response to tensile strain, in which case two valley Hall currents with opposite directions can be observed by injecting carriers with different spins into the system under the effect of an external electric field (Fig. 2(e)), which is expected to lead to the design of a new type of spin valley Hall device with high efficiency and low energy consumption. Subsequent reports indicate that doping/adsorption of transition metals is experimentally feasible and can acquire a large VP. For example, the experimental works of Li *et al.*, Zhou *et al.* and Ma *et al.* demonstrated the possibility of achieving VP in monolayer MoS_2 by doping magnetic atoms Fe, Co or Re, respectively.[61–63] Zhang *et al.* and Guo *et al.* obtained large VP of 83 meV and 108 meV by magnetic doping, respectively, and they predicted that AVHE can be achieved in these systems.[29,64]

3. Utilizing the magnetic proximity effect for VP and AVHE

VP and AVHE can be induced in 2D materials by doping with suitable transition metal atoms, but unfortunately there are very few ideal doping systems, and the properties of most doping systems are strongly influenced by the doped atoms, e.g., the introduced impurity energy levels can destroy the integrity of the valleys, which obviously hampers the application of valley degrees of freedom to the material. It is gratifying to note that the interfacial physics of 2D materials has attracted a lot of attention due to their atomically thin nature, and it has been found that the magnetic proximity effect of the system can be exploited to induce satisfying results by putting 2D materials on a magnetic substrate.[65] Therefore, it is possible to induce VP by building van der Waals heterostructures of 2D FM material and 2D valleytronic material with VHE, and such heterostructures with VP can be called as ferrovalley heterostructures. Considering that the external magnetic field only creates a small valley splitting, Qi *et al.* proposed that valley degeneracy can be lifted by the proximity-induced Zeeman effect in $MoTe_2$/EuO heterostructure and the AVHE can be achieved under hole doping.[46] Zhang *et al.* demonstrated that VP can be induced in $MoTe_2$/EuO(111) heterostructures by the magnetic proximity effect, and they designed valley filter and valley separator devices.[47] In 2016, Ye *et al.* succeeded in achieving the first successful electrical control of valley degree of freedom for electron, which opens up new possibilities for applications in the fields of valleytronics and spintronics.[66] The magnetic substrates that are able to be built into ferrovalley heterostructures include CrI_3, Cr_2O_3, T-$FeCl_2$, EuS, MnO, VSe_2, $Cr_2Ge_2Te_6$, etc.[49,52,67–71] For example, the group of Xiaodong Xu and their collaborators experimentally succeeded in preparing WSe_2/CrI_3 heterojunctions and achieved optical control.[72,73] The research on TMDs/CrI_3 heterostructures has also attracted much attention in theory.[50,51,53] However, the VP induced by the previously reported magnetic substrates is usually small (a few meV), which is not conducive to the application of valleytronics devices with AVHE, so the search for a new system of ferrovalley heterostructures is of important significance for the development of valleytronics.

3.1. H-Tl_2O/CrI_3 heterostructure

The monolayer CrI_3 with intrinsic magnetism, which is an out-of-plane Ising ferromagnet with a Curie temperature (T_C) of 45 K, has been successfully prepared experimentally by physical stripping in 2017.[74] The H-phase monolayer Tl_2O, with a structure similar to the TMDs with broken space-inversion symmetry, has been theoretically predicted to have a pair of degenerate valleys in both the conduction and valence bands.[75,76] Since VP can be generated only in the valence band of H-Tl_2O by doping with nonmetallic elements,[77] Guo *et al.* chose monolayer CrI_3 as a magnetic substrate to break the time-reversal symmetry of monolayer H-Tl_2O,[78] and thus observed the coexistence of VP in the conduction and valence bands. The configuration I is the most stable configuration because it has the lowest binding energy among the three stacking configurations. The calculations of the optimal stacking configuration (Fig. 3(a)) indicate the existence of a larger VP of 15.95 meV in the conduction band of the system under the influence of SOC with respect to the previously reported one, as shown in Fig. 3(b). Moreover, there is no significant valley annihilation of monolayer H-Tl_2O in Fig. 3(c), hence the H-Tl_2O/CrI_3 heterostructure is a promising material for spintronics and valleytronics applications.

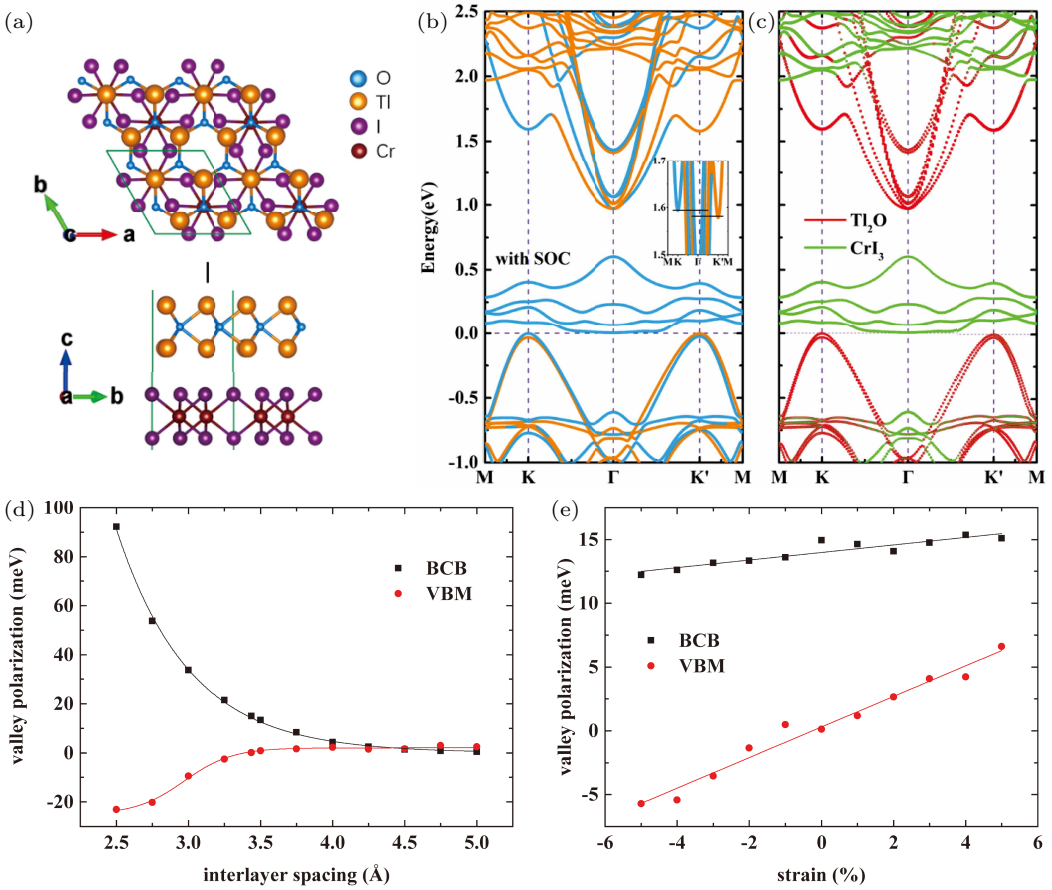


Fig. 3. (a) The top and side views of stacking configuration I for H-Tl_2O/CrI_3 heterostructure. (b) and (c) The spin-projected and atom-projected band structures of stacking configuration I for H-Tl_2O/CrI_3 heterostructure with SOC, where blue, orange, red and green lines represent the spin-up channel, spin-down channel, part of H-Tl_2O and CrI_3, respectively. (d) and (e) The VP in valence and conduction bands as functions of interlayer spacing and in-plane biaxial strain, respectively.[78]

Furthermore, it is desirable to obtain a larger and more experimentally operable VP by external modulation of the H-Tl_2O/CrI_3 heterostructure. The interfacial orbital hybridization of the heterostructure can be controlled by adjusting the interlayer spacing (Fig. 3(d)), so that the maximum VP values of 23.078 meV and 92.23 meV can be obtained in the valence and conduction bands, respectively. And under -5% to 5% in-plane biaxial strain in Fig. 3(e), the VP in both valence and conduction bands tends to increase. This research shows that it is feasible to induce VP in monolayer H-Tl_2O via the magnetic substrate monolayer CrI_3 and the H-Tl_2O/CrI_3 heterostructure is VP tunable, which provides a theoretical basis for applications of monolayer H-Tl_2O in valleytronics and provides new material system for the realization of AVHE.

3.2. TiX_2/CrI_3 and TiBrI/CrI_3 (X = Br, I) heterostructures

Zhao *et al.* followed up the previous work by choosing monolayer TiXY (X = Br, I) to continue to build ferrovalley heterostructures with experimentally synthesized monolayers CrI_3,[79] demonstrating that large VP can be induced by strong magnetic proximity effect, which is generated by the hybridization between monolayer TiXY and the magnetic substrate as well as by the magnetic exchange interaction

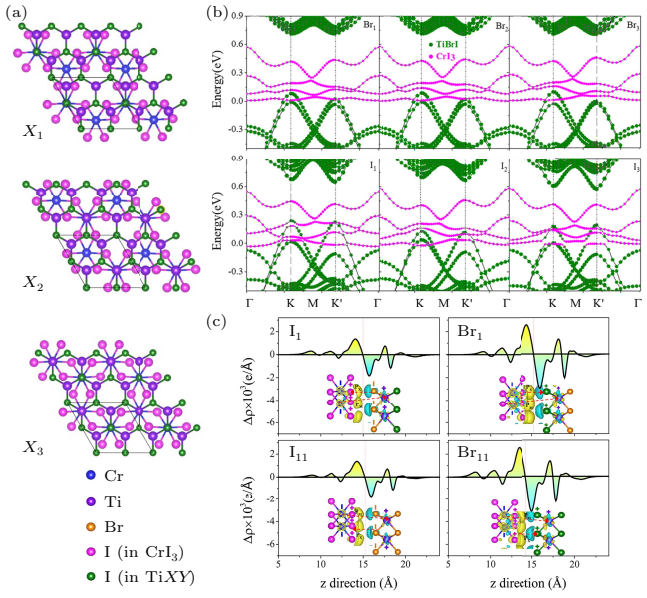


Fig. 4. (a) The top view of different stacking configuration for TiXY/CrI_3 heterostructure. (b) The atom-projected band structures of different stacking configurations for TiBrI/CrI_3 heterostructure with SOC, respectively. (c) Planar averaged charge density (upper part in each panel), side views of stacking configurations and differential charge density (lower part in each panel) for I_1, Br_1, I_{11}, and Br_{11}, respectively. P_M and P_X denote the interlayer electric polarization of Cr–Ti and I–I (Br). The yellow and cyan areas represent electron accumulation and depletion, respectively.[79]

between the layers. With the TiBrI/CrI_3 heterostructure as an example, it is calculated that all the stacking configurations (Fig. 4(a)) are the type-III band alignment in Fig. 4(b), which favors the charge transfer of TiBrI layer and CrI_3 layer. The dependence of the magnetic proximity effect on the stacking configuration is clearly reflected in the variation of the VP. The optimal stacking configuration for TiBrI/CrI_3 heterostructure is stacking I_1 with a VP of 16 meV. The VP of the stacking Br_1 formed after inversion of the TiBrI layer increases to 59 meV. The reason for this is that the strong magnetic field exchange interactions between the valleys of TiXY and the CrI_3 magnetic substrate due to magnetic proximity effects lead to a larger VP than in the conventional TMDs/CrI_3 system. The K and K' valleys in the conduction band of these systems that are not submerged by the CrI_3 layer possess significant VP that can realize AVHE. Furthermore, a comparison of TiBrI/CrI_3 with TiX_2/CrI_3 reveals that the crystal structure polarity also affects the VP (Fig. 4(c)), which in turn affects the AVHE. The detailed description of the various phenomena and the corresponding mechanisms of the constructed ferrovalley heterostructures was provided by Zhao *et al.* In addition, the investigated system TiBrI/CrI_3 has peculiar magneto-optical properties and can also be used as a transport channel for a type of spin field effect transistor. These findings have excellent potential for the development and innovation of spintronics, valleytronics, and nano-optics applications, and of course, especially for AVHE, materials that do not show significant valley annihilation and have a large VP would have even better performance.

3.3. HfNX (X = Cl, Br, I)/$FeCl_2$ heterostructure

The 2D magnetic semimetal 1T-$FeCl_2$, which can be successfully prepared by molecular-beam epitaxy, has a T_C of up to 160 K and super-exchange interactions.[80] Therefore, it is expected to be used as a magnetic substrate to induce VP instead of the conventional ferromagnetic (FM) monolayer CrI_3 with T_C of 45 K. The bulk material β-MNX (M = Zr, Hf; X = Cl, Br, I) with excellent optoelectronic and superconducting properties has been successfully synthesized for a long time.[81] Sun *et al.* built a ferrovalley heterostructure of the Janus material 1T-HfNX and the magnetic material 1T-$FeCl_2$, which was predicted to have a VP of 47.6 meV for its most stable stacking configuration resulting from a combination of magnetic proximity effect and SOC (Figs. 5(a) and 5(b)).[82] The VP above 100 meV can be obtained by both adjusting the layer spacing and applying biaxial strain in Figs. 5(d) and 5(e). Moreover, due to the super-exchange effect of the magnetic substrate 1T-$FeCl_2$, the VP of the HfNX/$FeCl_2$ heterostructure is robust, i.e., the valley signals of the system are non-volatile, which is beneficial for the application of valleytronics. Furthermore, the VP of the system is dependent on the magnetization direction of the magnetic substrate 1T-$FeCl_2$, as shown in Fig. 5(f). Applying a transverse electric field to such a system with VP, the Bloch electrons have Berry curvatures (Fig. 5(c)) of opposite sign and slightly different absolute values at the K and K' valleys, so that they acquire anomalous velocities in opposite directions. A net Hall current in the longitudinal direction can be obtained by shifting the Fermi energy level

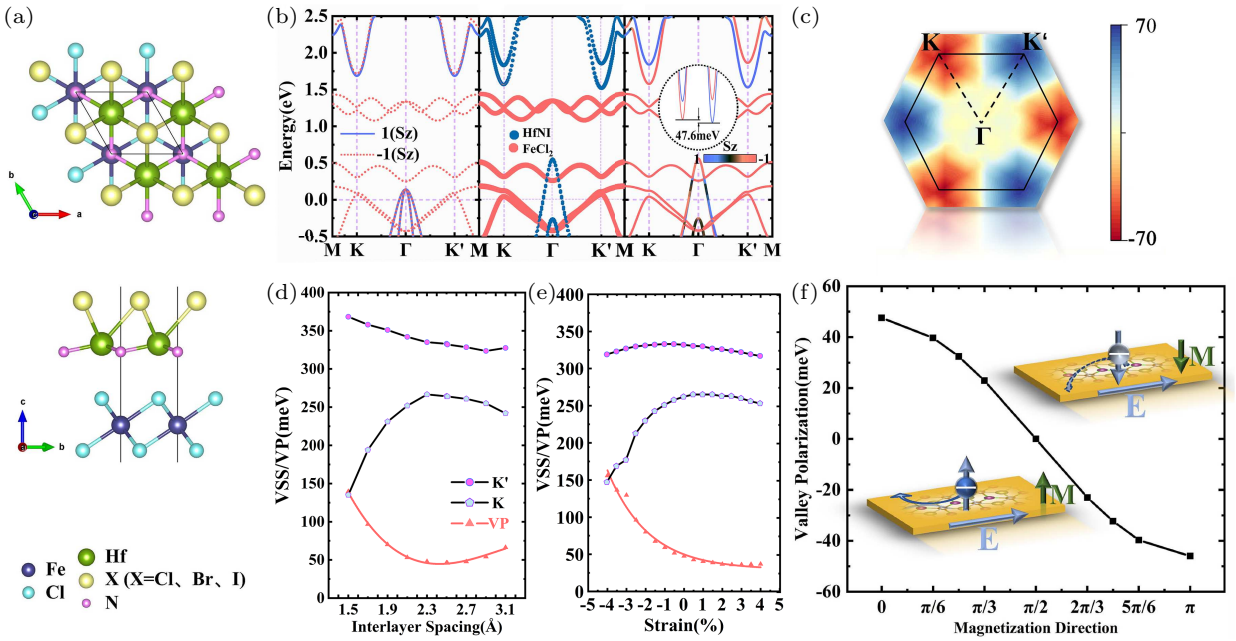


Fig. 5. (a) The top and side views of optimal stacking configuration for HfNX/$FeCl_2$ heterostructure. (b) The spin-projected band structure without SOC, atom-projected and the spin-projected band structures with SOC of optimal stacking configuration, respectively. (c) Berry curvature of optimal stacking configuration. (d) and (e) The curves of valley spin splitting and VP in conduction band with different interlayer spacings and in-plane biaxial strain of optimal stacking configuration, respectively. (f) Relationship between the VP and the magnetization direction and the illustration shows the AVHE.[82]

between the two valleys via electron doping or by applying a gate voltage, i.e., the AVHE (Fig. 5(f)) with a specified energy valley and spin index can be realized. Recently, some studies on magnetic proximity effects have been reported, such as heterostructures WSe_2/VSe_2 (VP of 19 meV) and CrI_3/MSi_2P_4 (M = Mo, W) (VP of a few meV).[83,84]

4. Intrinsic ferrovalley and external field modulation

In the pursuit of achieving VP and AVHE, various strategies have been proposed, yielding some promising results. However, it should not be overlooked that these methods also have drawbacks to some extent. For instance, the application of external electromagnetic fields can lead to VP instability, which may affect the reproducibility of the experiment.[36–39] Additionally, the precise control of optical pumping is a challenge in achieving VP, and magnetic doping methods may introduce impurity energy levels that can affect the electronic properties of the material.[33–35,41–44] Lastly, the magnetic proximity effect may result in a small VP, limiting its application of AVHE.[45–54,84] Furthermore, it is important to note that only a very limited number of 2D materials exhibiting VP characteristics have been successfully prepared in experiments.[61–63,66,72,73,85] If we continue to rely solely on these methods, it will impede the advancement of spintronics and valleytronics. Therefore, it is necessary to further search for new approaches to overcome these limitations and achieve more stable and controllable VP to advance AVHE in these fields.

Tong *et al.* in 2016 proposed an important research paradigm, wherein VP can spontaneously occur in certain 2D hexagonal honeycomb lattice materials with both broken time-reversal symmetry and space-inversion symmetry.[31] The spontaneous VP makes the material nonvolatile for data storage. Such materials can realize the AVHE and are referred to as ferrovalley materials. This discovery circumvents the drawbacks of conventional methods for generating VP in terms of volatility, weak transport, and low resource utilization, which opens up new research avenues and holds significant importance for understanding and using the potential applications of VP and AVHE in spintronics and valleytronics. More excitingly, Wang *et al.* reported experimentally that 2H-phase VSe_2 at 2D limit is a room-temperature ferromagnetic semiconductor, and You *et al.* successfully obtained H-phase monolayer VSe_2 on a mica substrate by the chemical vapor deposition method.[86,87] These provide a potential for the experimental synthesis and application of ferrovalley materials.

4.1. Ferrovalley Janus 1T-CrOX (X = F, Cl, Br, I) and the multiferroic heterostructure CrOX/In_2Se_3

Some 2D ferrovalley materials, such as H-$FeCl_2$, Nb_3I_8, GdI_2 and NdX_2, have been theoretically predicted to exhibit non-volatile VP due to the interplay between their inherent magnetic exchange fields and SOC.[88–91] Most of these reported 2D ferrovalley materials belong to the H-phase structure. Inspired by that, Sun *et al.* predicted a 2D T-phase Janus material called CrOX (X = F, Cl, Br, I), whose lattice structure is shown in Fig. 6(a).[92] It can be observed from Figs. 6(b) and 6(c) that CrOCl with T_C of 85 K and CrOBr with T_C of 17 K belong to the ferrovalley materials. They exhibit spontaneous VPs of 33 meV and 54 meV in the conduction band and 8 meV and 44 meV in the valence band, respectively. These materials are expected to be used in valleytronics devices in the future due to their T_C close to the T_C of CrI_3, which has been successfully synthesized.

Sun *et al.* used a SOC effective model to give an intrinsic mechanism for the production of VP in the 1T-CrOX system, and the corresponding equations are shown as follows:[92,93]

$$\hat{H}_{\rm SOC} \approx \hat{H}^0_{\rm SOC} = \lambda \hat{S}_{z'}(\hat{L}_z \cos\theta + \frac{1}{2}\hat{L}_+ \mathrm{e}^{-\mathrm{i}\phi}\sin\theta + \frac{1}{2}\hat{L}_- \mathrm{e}^{+\mathrm{i}\phi}\sin\theta), \tag{1}$$

$$\hat{L}_+ = \hat{L}_x + \mathrm{i}\hat{L}_y, \quad \hat{L}_- = \hat{L}_x - \mathrm{i}\hat{L}_y, \tag{2}$$

$$|\psi_{\rm v}\rangle = |d_{z^2}\rangle, \quad |\psi^\tau_{\rm c}\rangle = \sqrt{\frac{1}{2}}(|d_{x^2-y^2}\rangle + \mathrm{i}\tau|d_{xy}\rangle, \tag{3}$$

$$E_{\rm v} = \langle\psi_{\rm v}|\hat{H}_{\rm SOC}|\psi_{\rm v}\rangle, \quad E^\tau_{\rm c} = \langle\psi^\tau_{\rm c}|\hat{H}_{\rm SOC}|\psi^\tau_{\rm c}\rangle, \tag{4}$$

$$E_{\rm c} - E'_{\rm c} = \mathrm{i}\langle d_{x^2-y^2}|\hat{H}_{\rm SOC}|d_{xy}\rangle - \mathrm{i}\langle d_{xy}|\hat{H}_{\rm SOC}|d_{x^2-y^2}\rangle \propto 4\cos\theta, \tag{5}$$

$$E_{\rm v} - E'_{\rm v} \approx 0, \tag{6}$$

where λ, $\hat{L}$, and $\hat{S}$ represent the strength of the SOC effect, the orbital angular momentum, and the spin angular momentum, respectively. Both θ and ϕ are the magnetocrystalline angles. It is worth noting that θ is zero along the z direction and ϕ is zero along the x direction. (x,y,z) and (x',y',z') are the coordinate systems of $\hat{L}$ and $\hat{S}$, respectively. $|\psi_{\rm v}\rangle$ and $|\psi^\tau_{\rm c}\rangle$ are the basic functions. $\tau = \pm 1$ represent the valley index. The results of Eqs. (5) and (6) are consistent with the energy band structure calculations of the Heyd–Scuseria–Ernzerhof density functional. Therefore, the spontaneous VP in CrOCl and CrOBr can lead to AVHE, which means that the Bloch electrons will acquire anomalous velocities $\boldsymbol{v}_\perp \sim \boldsymbol{E} \times \boldsymbol{\Omega}_z(\boldsymbol{k})$ in the presence of an applied transverse electric field, and the Fermi energy levels can be shifted between the two valleys in the conduction band by doping the electrons, which will result in the spin-up electrons from the K' valleys gathering on one boundary of the material, thus achieving AVHE.

Under external modulation, the calculated results, as shown in Figs. 6(d) and 6(e), indicate that the variation of VP with θ is consistent with the theoretical prediction of Eq. (5). The VP of CrOCl in Fig. 6(f) is robust to biaxial strain due to the relatively small range of variation. However, the VP in conduction band increases with biaxial strain in CrOBr, while

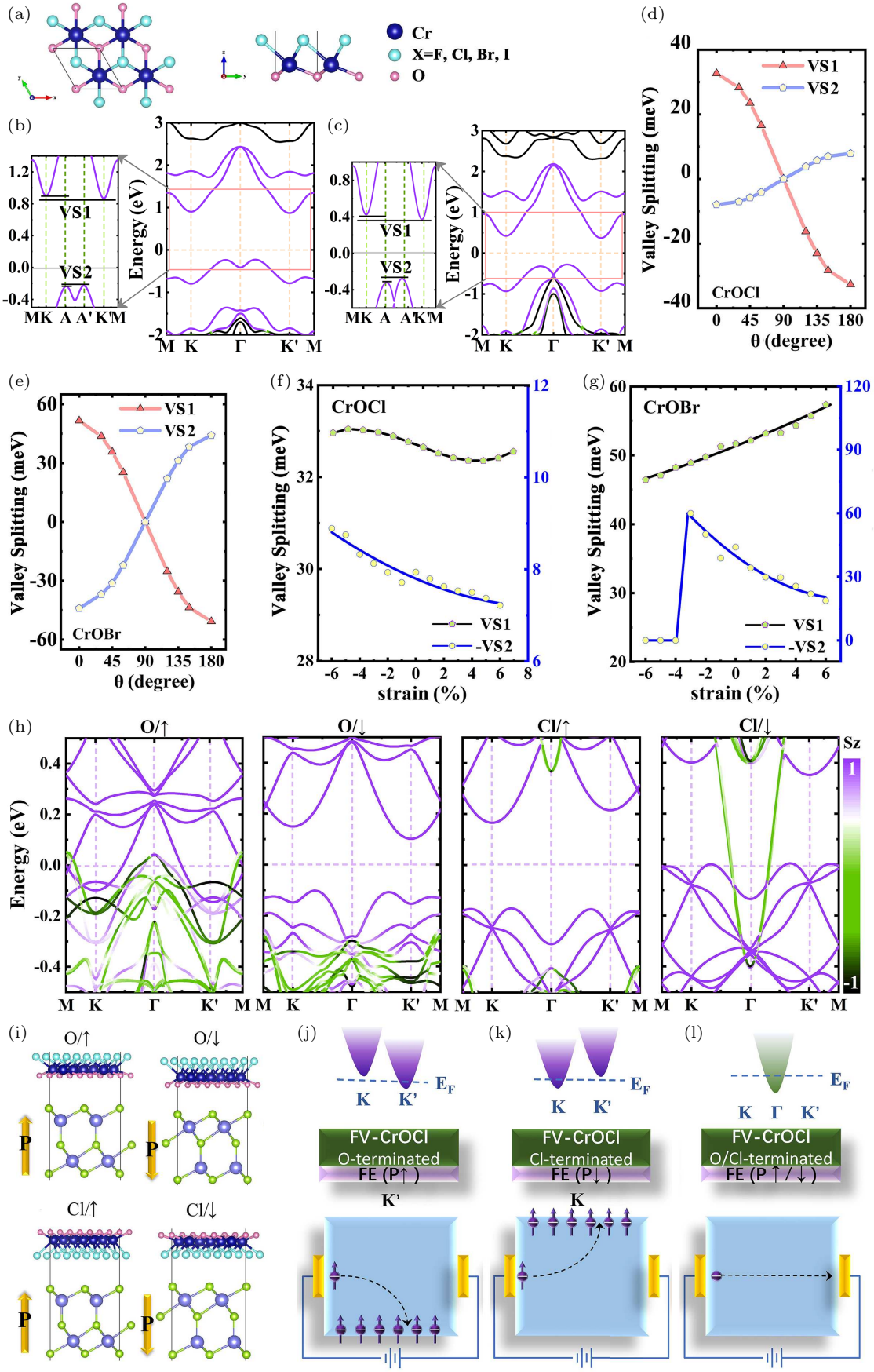


Fig. 6. (a) The top and side views of monolayer 1T-CrOX (X = F, Cl, Br, I). (b) and (c) The spin-projected band structures of 1T-CrOCl and 1T-CrOBr with SOC, respectively. (d) and (e) The VP in valence and conduction bands as functions of θ for 1T-CrOCl and 1T-CrOBr, respectively. (f) and (g) The VP in valence and conduction bands as functions of biaxial strain for 1T-CrOCl and 1T-CrOBr, respectively. (h) and (i) The spin-projected band structures and the structures of SOC for the multiferroic heterostructures CrOX/In_2Se_3. (j)–(l) The schematics of the reversible switching of AVHE in different systems.[92]

the VP in valence band exhibits a switching effect, as shown in Fig. 6(g). These results are important for relevant applications in the field of valleytronics. In addition, the application of near-field effects can lead to exciting phenomena due to the atomic-level thinness of 2D materials.[94–97] 2D ferroelectric materials with stable spontaneous polarization have attracted extensive attention in recent years.[98–101] A heterostructure is built using a ferroelectric substrate and a 2D valleytronics material to achieve nonvolatile control of valleytronics, which contributes to the design of novel controllable nonvolatile ferroelectric memory devices. Sun *et al.* successfully achieved switchable switching with VP (Figs. 6(h) and 6(i)) using a 1T-CrOCl ferrovalley material in combination with a synthesized In_2Se_3 ferroelectric material. Figures 6(j)–6(l) show the schematics of the reversible switching of AVHE under in-plane electric field. This discovery is expected to advance the field of valleytronics by exploiting the duality of valley degrees of freedom to help develop read–write non-volatile storage devices. Recently, a real heterostructure of VSe_2/Al_2S_3 is predicted theoretically by Lei *et al.*, the AVHE in VSe_2 can be stably preserved under the modulation of the ferroelectric substrate Al_2S_3.[102] These studies of ferroelectric-valley coupling have enriched and advanced the field related to 2D valley electronics materials and ferroelectrics.[103]

4.2. Janus monolayer Fe_2SSe

The studied systems that can realize VP are usually broken in both space-inversion symmetry and time-reversal symmetry, in this case, a valley-polarized quantum anomalous Hall effect (VP-QAHE), also known as quantum anomalous valley Hall effect, that combines the valley index with the quantum anomalous Hall effect is proposed, and the proposal of this effect brings new research directions and possibilities in the field of valleytronics, which is significant for the development of new electronic devices and materials.[22,104–110] Recently, Li *et al.* theoretically predicted that monolayer Fe_2X_2 (X = S,Se) materials with hexagonal honeycomb lattice structures are intrinsically magnetic topological insulators with large nontrivial gap and high T_C.[111] In order to achieve the intrinsic VP-QAHE, Chen *et al.* took a key initiative to construct a monolayer Janus material, Fe_2SSe (Fig. 7(a)), through which the VP was introduced by breaking the space-inversion symmetry of Fe_2X_2.[112] The monolayer Fe_2SSe exhibits spontaneous VP of 5 meV in the conduction band and 18 meV in the valence band (Fig. 7(b)) and a SOC effective model is given to explain the mechanism of VP generation. The edge states of the system form chiral–spin–valley locking edge states under the modulation of the magnetization orientation due to the existence of valleys in Figs. 7(c) and 7(d). This implies that a locking relationship is formed between the edge states, spins, and valleys of the system under a particular magnetization orientation, exhibiting chiral characteristics. In addition, abundant phase transition phenomena can be realized by external field modulation (Figs. 7(e) and 7(f)). For example, a ferrovalley material with a spontaneous VP of 52 meV can be obtained under a tensile strain with a strain rate of 8% at $U = 3$. And the results of this study show that the intrinsic VP-QAHE can be achieved in specific material designs and constructions, which offer a novel electronic devices and materials development, providing potential avenues.

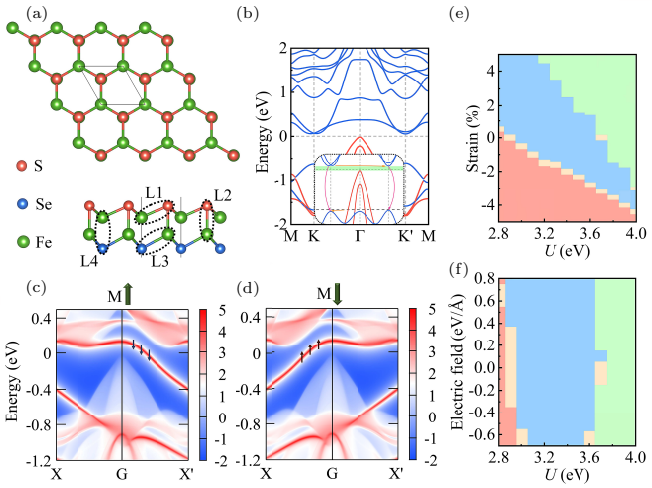


Fig. 7. (a) The top and side views of Janus monolayer Fe_2SSe. (b) The spin-projected band structures of Janus monolayer Fe_2SSe with SOC, where the blue, red lines and the light green area represent the spin-up channel, spin-down channel and the band gap, respectively. (c) and (d) The chiral edge states of Janus monolayer Fe_2SSe under different magnetization orientations. (e) and (f) Phase diagram dependent on U values and biaxial strain or electric field. The red, yellow, blue, and green areas indicate that the system is in metal, half-metal, magnetic topological insulator, and ferrovalley phases, respectively.[112]

4.3. $MHfN_2Cl_2$ (M = V, Cr) bimetallic nitrogen halide monolayers

The presence of weak van der Waals interactions between the multi-metal layered transition metal nitride halides (TMNHs) bulk materials of types α and β allows them to be easily exfoliated into monolayers.[113] The synthesized β-type $Hf_2N_2Cl_2$ material cannot be used in spintronics and energy valleytronics devices due to its nonmagnetic properties.[114,115] In order to introduce magnetism and break the spatial inversion symmetry, Sun *et al.* employed V or Cr atoms instead of monolayer Hf atoms (Fig. 8(a)) and predicted T_C of 104 K and 36 K for the monolayer ferrovalley material $MHfN_2Cl_2$ (M = V, Cr), respectively.[116] Figure 8(b) shows that the half-metal $VHfN_2Cl_2$ has only a spontaneous VP of 16 meV far from the Fermi energy level at the conduction band, which limits its usefulness in practical applications. In contrast, $CrHfN_2Cl_2$ is an excellent ferrovalley material, possessing a spontaneous VP up to 55 meV in Fig. 8(c). The production mechanism of its spontaneous VP is also successfully explained by the effective SOC model developed by Sun *et al*. In addition, the results of Berry curvature (Fig. 8(d)) and

anomalous Hall conductivity (Fig. 8(e)) show that $CrHfN_2Cl_2$ can realize AVHE. In addition, the biaxial strain and U values can effectively modulate the VP (Figs. 8(f)–8(i)) and T_C of $MHfN_2Cl_2$, especially for half-metal $VHfN_2Cl_2$, which can realize the valley switching in its conduction band. This work provides a new direction for the search of ferrovalley materials, which is expected to play an important role in spintronics and valleytronics devices.

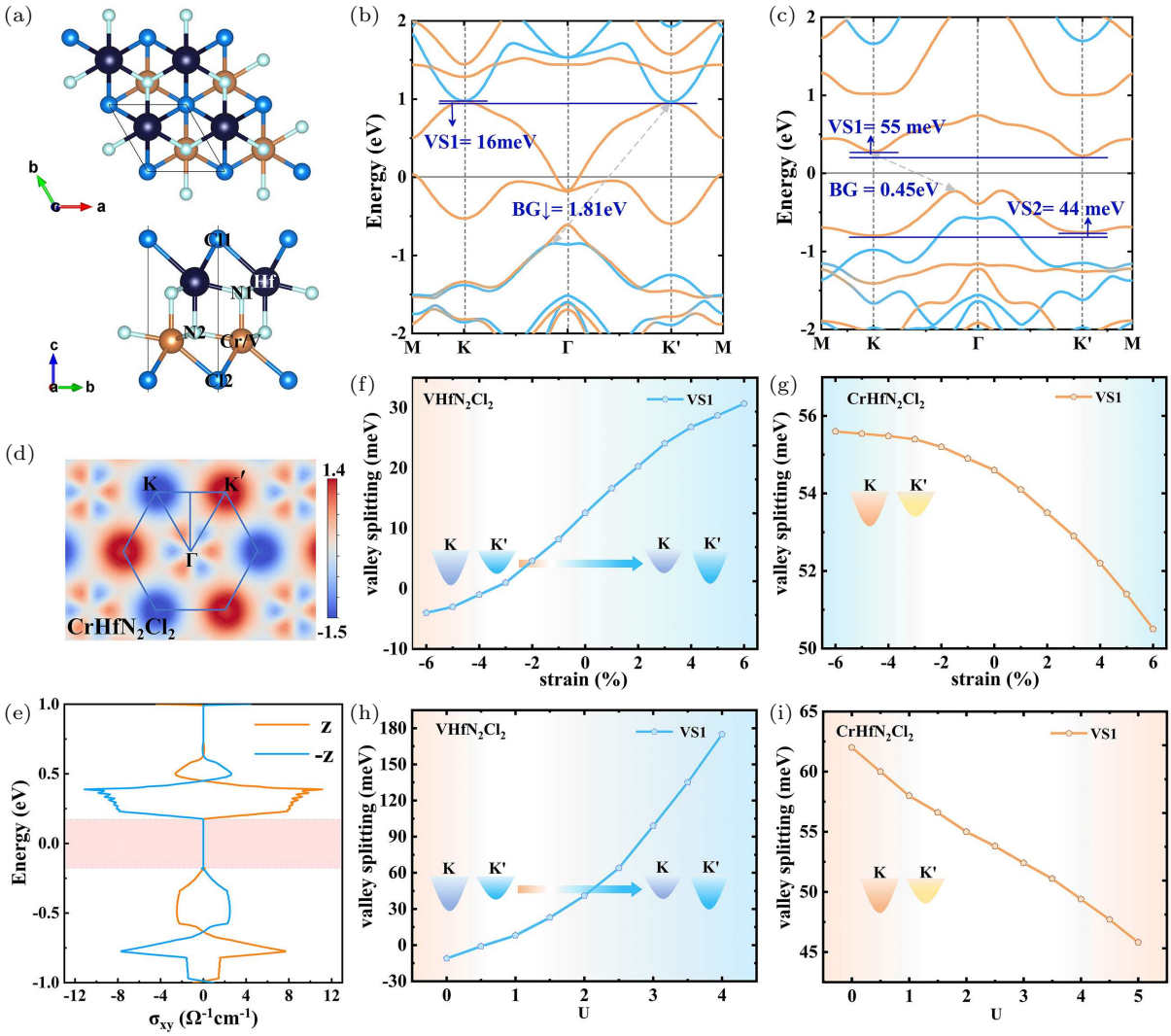


Fig. 8. (a) The top and side views of monolayer $MHfN_2Cl_2$ (M = V, Cr). (b) and (c) The spin-projected band structures of monolayer $VHfN_2Cl_2$ and $CrHfN_2Cl_2$ with SOC, where blue and orange lines represent the spin-up channel and spin-down channel, respectively. (d) and (e) The Berry curvature and anomalous Hall conductivity of monolayer $CrHfN_2Cl_2$, respectively. The VP in conduction band as functions of biaxial strain (f) and (g) and U value (h) and (i) for monolayer $VHfN_2Cl_2$ and $CrHfN_2Cl_2$, respectively.[116]

4.4. MXene monolayer $M_3N_2O_2$ (M = Y, La)

The paucity of experimental materials with spontaneous VP, most of which are 2D TMDs and their Janus structures, and the fact that some material systems are limited by in-plane magnetic easy axis restrict the diversity of materials that can be used for AVHE.[31,90,117,118] Therefore, it is necessary to break the current mindset of searching for new materials with spontaneous VP. MXene materials are excellent for this purpose.[119–124] Lu *et al.* predicted a class of monolayer MXene materials $M_3N_2O_2$ (M = Y, La) (Fig. 9(a)) with spontaneous VP.[125] Under the combined effect of SOC and intrinsic magnetic moments, monolayer $Y_3N_2O_2$ obtains a spontaneous VP of 21.3 meV in the conduction band as shown in Fig. 9(b). The corresponding mechanism of VP generation is given by a SOC efficient model. The K and K' valleys exhibit different absolute values and opposite signs of the Berry curvature in Fig. 9(c), which implies that the Bloch electrons can acquire anomalous velocities in the presence of an external electric field, resulting in AVHE. When the magnetization direction of the system is reversed, the AVHE changes accordingly (Fig. 9(d)). However, the intrinsic VP of monolayer $Y_3N_2O_2$ is relatively small. In order to enhance the VP, Lu *et al.* adopted different external modulations, and their results showed that increasing the strength of SOC could lead to a larger VP in Fig. 9(e). Therefore, they choose to replace the Y atoms with heavier La atoms in order to introduce a stronger

SOC, and finally achieve a spontaneous VP up to 100.4 meV in monolayer $La_3N_2O_2$ (Fig. 9(f)), which provides the possibility of experimental observation and practical application of AVHE. This work not only provides new ferrovalley materials, but also offers new ideas for obtaining large spontaneous VP, which promotes the development process of valleytronics devices.

Ferrovalley materials that can exist at high temperatures and possess large VP are highly expected in the current condensed matter physics research. Recently, some novel ferrovalley materials have been reported, for instance, the large VP of 67 meV, 108.98 meV, 93 meV, 90 meV, and 226 meV are predicted in monolayers $Fe(OH)_2$, YX_2, ScI_2, ScBrI, and RuClBr with magnetic moment along the z direction, respectively.[126–130] Excitingly, the large VP is beneficial for achieving AVHE at room temperature, which provides material bases for the development of valley electronics and opens new avenues for exploring new electronics and nanotechnology applications using valley degrees of freedom. In addition, much attention has been focused on the diverse modulation of ferrovalley materials, such as the modulation of ferrovalley bilayers, the AVHE can be modulated by changing the direction of the applied vertical electric field in antiferrovalley bilayer VSe_2, 3R-type antiferromagnetic bilayers VS_2 and YI_2, as well as antiferromagnetic bilayer and triple-layer T-$FeCl_2$ due to the ferroelectricity-valley coupling.[131–134] Moreover, Li *et al.* achieved the structure-controlled AVHE in the VSe_2/VSeX (X = S, Te) heterostructures.[135] They also investigated the mechanism of AVHE in monolayer OsClBr and found that VP-QAHE can be obtained and modulated by forming bilayer or applying strain in OsClBr.[136] These studies will help drive scientific and technological advances in various fields and offer promising prospects for future applications and innovations.

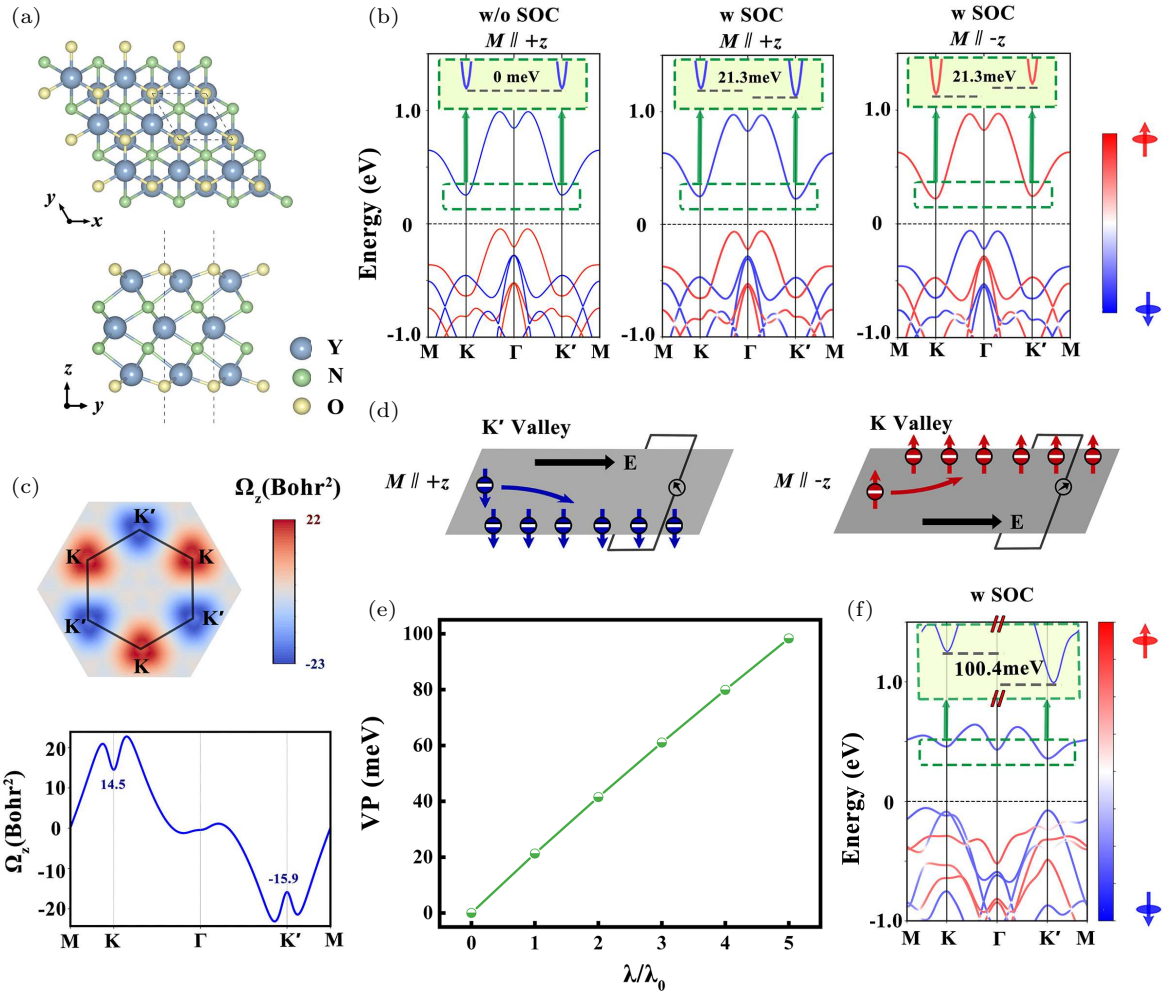


Fig. 9. (a) The top and side views of MXene monolayer $Y_3N_2O_2$. The spin-projected band structures (b), the Berry curvature (c) and the schematics of AVHE (d) for monolayer $Y_3N_2O_2$. (e) The VP in conduction band as functions of the strength of SOC for monolayer $Y_3N_2O_2$. (f) The spin-projected band structure of monolayer $La_3N_2O_2$ with SOC.[125]

5. Conclusion and outlook

This review describes several methods for achieving AVHE, emphasizing the importance of VP in 2D materials. Doping or adsorption of transition metal atoms to monolayer TMDs and Janus materials can obtain VP and the magnitude of VP can be adjusted by the type of transition metal atoms,

but unfortunately the application of VP and AVHE is hindered in most doping or adsorption systems by the fact that the impurity energy levels are located near the Fermi energy. Building 2D valleytronics materials protected by time-reversal symmetry on FM substrate materials can introduce VP by magnetic proximity effects. However, the relatively small intrinsic VP produced by ferrovalley heterostructures is not conducive to practical applications of AVHE, which led researchers to shift their attention to ferrovalley materials possessing spontaneous VP. Furthermore, the external conditions exerted on the 2D ferrovalley system can modulate AVHE to make it easier to be applied, and some exotic properties can be obtained, such as AVHE switching, VP-QAHE, and ferroelectric-valley coupling. These researches not only advance AVHE in the field of valleytronics, but also promote the integration of valleytronics with ferroelectrics or topology.

AVHE, the fundamental transport phenomenon, has particular potential in the field of novel electronic devices and can be used in many applications. For example, different VP states in 2D valleytronic materials can be used to encode and store information, which provides the possibility of applying 2D valleytronic materials to future novel electronic devices with low energy consumption and rich functionality. Up to now, many significant advances have been made in the field of valleytronics. In addition to the search for more readily synthesized and more experimentally applicable valleytronic materials with VP and AVHE, exploring a variety of external controls over them is also important. Valleytronics has also integrated with other research fields and achieved significant progress, such as photonics, new energy sources, and topological materials, which holds the promise of low-energy-consuming devices in the future. Although theoretical and experimental researches in the field of valleytronics are booming, there exists the demand for further searching and enrichment of experimentally feasible valleytronic materials that can be promoted for practical applications.

Acknowledgments

Project supported by the National Natural Science Foundation of China (Grant Nos. 12274264 and 11674197), the Natural Science Foundation of Shandong Province of China (Grant Nos. ZR2022MA039 and ZR2021MA105), and the Qing-Chuang Science and Technology Plan of Shandong Province of China (Grant No. 2019KJJ014).

References

[1] Novoselov K S, Geim A K, Morozov S V, Jiang D, Zhang Y, Dubonos S V, Grigorieva I V and Firsov A A 2004 *Science* **306** 666
[2] Geim A K and Novoselov K S 2007 *Nat. Mater.* **6** 183
[3] Mas-Ballesté R, Gómez-Navarro C, Gómez-Herrero J and Zamora F 2011 *Nanoscale* **3** 20
[4] Lebègue S, Björkman T, Klintenberg M, Nieminen R M and Eriksson O 2013 *Phys. Rev. X* **3** 031002
[5] Fiori G, Bonaccorso F, Iannaccone G, *et al.* 2014 *Nat. Nanotechnol.* **9** 768
[6] Bhimanapati G R, Lin Z, Meunier V, *et al.* 2015 *ACS Nano* **9** 11509
[7] Morozov S V, Novoselov K S, Katsnelson M I, Schedin F, Ponomarenko L A, Jiang D and Geim A K 2006 *Phys. Rev. Lett.* **97** 016801
[8] Morpurgo A F and Guinea F 2006 *Phys. Rev. Lett.* **97** 196804
[9] Gorbachev R V, Tikhonenko F V, Mayorov A S, Horsell D W and Savchenko A K 2007 *Phys. Rev. Lett.* **98** 176805
[10] Rycerz A, Tworzydło J and Beenakker C 2007 *Nat. Phys.* **3** 172
[11] Xiao D, Yao W and Niu Q 2007 *Phys. Rev. Lett.* **99** 236809
[12] Schaibley J R, Yu H, Clark G, *et al.* 2016 *Nat. Rev. Mater.* **1** 16055
[13] Wang Q H, Kalantar-Zadeh K, Kis A, Coleman J N and Strano M S 2012 *Nat. Nanotechnol.* **7** 699
[14] Ajayan P, Kim P and Banerjee K 2016 *Phys. Today* **69** 38
[15] Novoselov K S, Mishchenko A, Carvalho A and Castro Neto A H 2016 *Science* **353** aac9439
[16] Manzeli S, Ovchinnikov D, Pasquier D, Yazyev O V and Kis A 2017 *Nat. Rev. Mater.* **2** 17033
[17] Li P, Cui J, Zhou J, *et al.* 2020 *Chin. Sci. Bull.* **65** 882
[18] Xiao D, Liu G B, Feng W, Xu X and Yao W 2012 *Phys. Rev. Lett.* **108** 196802
[19] Saito Y, Nakamura Y, Bahramy M S, *et al.* 2016 *Nat. Phys.* **12** 144
[20] Dey P, Yang L, Robert C, *et al.* 2017 *Phys. Rev. Lett.* **119** 137401
[21] Mak K F, McGill K L, Park J and McEuen P L 2014 *Science* **344** 1489
[22] Pan H, Li Z, Liu C C, Zhu G, Qiao Z and Yao Y 2014 *Phys. Rev. Lett.* **112** 106802
[23] Xu X, Yao W, Xiao D and Heinz T F 2014 *Nat. Phys.* **10** 343
[24] Wang Y, Wei W, Wang H, *et al.* 2019 *J. Phys. Chem. Lett.* **10** 7426
[25] Gong J, Lin Z, Ye G L, *et al.* 2015 *ACS Nano* **9** 11658
[26] Li L, Shao L, Liu X, *et al.* 2020 *Nat. Nanotechnol.* **15** 743
[27] Dou K, Ma Y, Peng R, Du W, Huang B and Dai Y 2020 *Appl. Phys. Lett.* **117** 172405
[28] Li S, Wu W, Feng X, Guan S, Feng W, Yao Y and Yang S A 2020 *Phys. Rev. B* **102** 235435
[29] Guo J, Lu Z, Wang K, Zhao X, Hu G, Yuan X and Ren J 2022 *J. Phys.: Condens. Matter* **34** 075701
[30] Zeng H L and Cui X D 2016 *Physics* **45** 505
[31] Tong W Y, Gong S J, Wan X and Duan C G 2016 *Nat. Commun.* **7** 13612
[32] Akhmerov A R and Beenakker C W J 2007 *Phys. Rev. Lett.* **98** 157003
[33] Takashina K, Ono Y, Fujiwara A, Takahashi Y and Hirayama Y 2006 *Phys. Rev. Lett.* **96** 236801
[34] Bishop N C, Padmanabhan M, Vakili K, Shkolnikov Y P, De Poortere E P and Shayegan M 2007 *Phys. Rev. Lett.* **98** 266404
[35] Zeng H, Dai J, Yao W, Xiao D and Cui X 2012 *Nat. Nanotechnol.* **7** 490
[36] Mak K F, He K, Shan J and Heinz T F 2012 *Nat. Nanotechnol.* **7** 494
[37] Sie E J, McIver J W, Lee Y H, Fu L, Kong J and Gedik N 2015 *Nat. Mater.* **14** 290
[38] Li Y, Ludwig J, Low T, *et al.* 2014 *Phys. Rev. Lett.* **113** 266804
[39] Srivastava A, Sidler M, Allain A V, Lembke D S, Kis A and Imamoglu A 2015 *Nat. Phys.* **11** 141
[40] Aivazian G, Gong Z, Jones A M, Chu R L, Yan J, Mandrus D G, Zhang C, Cobden D, Yao W and Xu X 2015 *Nat. Phys.* **11** 148
[41] MacNeill D, Heikes C, Mak K F, Anderson Z, Kormányos A, Zólyomi V, Park J and Ralph D C 2015 *Phys. Rev. Lett.* **114** 037401
[42] Cheng Y C, Zhang Q Y and Schwingenschlögl U 2014 *Phys. Rev. B* **89** 155429
[43] Chen X, Zhong L S, Li X and Qi J S 2017 *Nanoscale* **9** 2188
[44] Peng R, Ma Y, Zhang S, Huang B and Dai Y 2018 *J. Phys. Chem. Lett.* **9** 3612
[45] Feng S, Cong C, Konabe S, *et al.* 2019 *Small* **15** 1805503
[46] Qi J, Li X, Niu Q and Feng J 2015 *Phys. Rev. B* **92** 121403
[47] Zhang Q, Yang S A, Mi W, Cheng Y and Schwingenschlögl U 2016 *Adv. Mater.* **28** 959
[48] Norden T, Zhao C, Zhang P, Sabirianov R, Petrou A and Zeng H 2019 *Nat. Commun.* **10** 4163
[49] Zhang Z, Ni X, Huang H, Hu L and Liu F 2019 *Phys. Rev. B* **99** 115441
[50] Zollner K, Junior P E F and Fabian J 2019 *Phys. Rev. B* **100** 085128
[51] Zhai B, Du J, Shen C, Wang T, Peng Y, Zhang Q and Xia C 2019 *Phys. Rev. B* **100** 195307
[52] Zhang K, Wang L and Wu X 2019 *Nanoscale* **11** 19536

[53] Hu T, Zhao G, Gao H, Wu Y, Hong J, Stroppa A and Ren W 2020 *Phys. Rev. B* **101** 125401
[54] Lei C, Ma Y, Zhang T, Xu X, Huang B and Dai Y 2020 *New J. Phys.* **22** 033002
[55] Zhang H, Yang W, Ning Y and Xu X 2020 *Phys. Rev. B* **101** 205404
[56] Cheng Y C, Zhu Z Y, Mi W B, Guo Z B and Schwingenschlögl U 2013 *Phys. Rev. B* **87** 100401
[57] Er D, Ye H, Frey N C, *et al.* 2018 *Nano Lett.* **18** 3943
[58] Xia C X, Xiong W Q, Du J, Wang T X, Peng Y T and Li J B 2018 *Phys. Rev. B* **98** 165424
[59] Zhao X W, Qiu B, Hu G C, Yue W W, Ren J F and Yuan X B 2019 *Appl. Surf. Sci.* **490** 172
[60] Zhao X W, Li Y, Liang R D, Hu G C, Yuan X B and Ren J F 2020 *Appl. Surf. Sci.* **504** 144367
[61] Li Q, Zhao X, Deng L, *et al.* 2020 *ACS Nano* **14** 4636
[62] Zhou J, Lin J, Sims H, *et al.* 2020 *Adv. Mater.* **32** 1906536
[63] Ma X, Zhang J, Lai J, Zhang M, Zheng J, Wu S, Hu X, Wang Q, Gan X, Sun D and Liu J 2021 *2D Mater.* **8** 035031
[64] Zhang T, Ma Y, Xu X, Lei C, Huang B and Dai Y 2020 *J. Phys. Chem. C* **124** 20598
[65] Yang H X, Hallal A, Terrade D, Waintal X, Roche S and Chshiev M 2013 *Phys. Rev. Lett.* **110** 046603
[66] Ye Y, Xiao J, Wang H, Ye Z, Zhu H, Zhao M, Wang Y, Zhao J, Yin X and Zhang X 2016 *Nat. Nanotechnol.* **11** 598
[67] Song Y, Li D, Mi W B, Wang X C and Cheng Y C 2016 *J. Phys. Chem. C* **120** 5613
[68] Liang X, Deng L, Huang F, Tang T, Wang C, Zhu Y, Qin J, Zhang Y, Peng B and Bi L 2017 *Nanoscale* **9** 9502
[69] Xu L, Yang M, Shen L, Zhou J, Zhu T and Feng Y P 2018 *Phys. Rev. B* **97** 041405
[70] Yu W, Li J, Herng T S, *et al.* 2019 *Adv. Mater.* **31** 1903779
[71] Dong X J, You J Y, Gu B and Su G 2019 *Phys. Rev. Appl.* **12** 014020
[72] Zhong D, Seyler K L, Linpeng X, *et al.* 2017 *Sci. Adv.* **3** e1603113
[73] Seyler K L, Zhong D, Huang B, *et al.* 2018 *Nano Lett.* **18** 3823
[74] Huang B, Clark G, Navarro-Moratalla E, *et al.* 2017 *Nature* **546** 270
[75] Ma Y, Kuc A and Heine T 2017 *J. Am. Chem. Soc.* **139** 11694
[76] Ma Y, Kou L, Du A, Huang B, Dai Y and Heine T 2018 *Phys. Rev. B* **97** 035444
[77] Xu X, Ma Y, Zhang T, Lei C, Huang B and Dai Y 2019 *J. Phys. Chem. Lett.* **10** 4535
[78] Guo J T, Zhao X W, Hu G C, Ren J F and Yuan X B 2021 *Appl. Surf. Sci.* **558** 149604
[79] Zhao X, Liu F, Ren J and Qu F 2021 *Phys. Rev. B* **104** 085119
[80] Zhong D Y, Drzewinski A, Zhou X H, *et al.* 2020 *J. Phys. Chem. C* **124** 9416
[81] Yamanaka S, Itoh K, Fukuoka H and Yasukawa M 2000 *Inorg. Chem.* **39** 806
[82] Sun R J, Lu J J, Zhao X W, Hu G C, Yuan X B and Ren J F 2022 *Appl. Phys. Lett.* **120** 063103
[83] Marfoua B and Hong J 2022 *Commun. Phys.* **5** 266
[84] Qi Y, Yao C and Zhao J 2023 *Phys. Rev. B* **108** 125304
[85] Wen T, Zhang W, Liu S, Hu A, Zhao J, Ye Y, Chen Y, Qiu C W, Gong Q and Lu G 2020 *Sci. Adv.* **6** eaao0019
[86] Wang X, Li D, Li Z, Wu C, Che C M, Chen G and Cui X 2021 *ACS Nano* **15** 16236
[87] You J, Pan J, Shang S L, *et al.* 2022 *Nano Lett.* **22** 10167
[88] Hu H, Tong W Y, Shen Y H, Wan X and Duan C G 2020 *NPJ Comput. Mater.* **6** 129
[89] Peng R, Ma Y, Xu X, He Z, Huang B and Dai Y 2020 *Phys. Rev. B* **102** 035412
[90] Cheng H X, Zhou J, Ji W, Zhang Y N and Feng Y P 2021 *Phys. Rev. B* **103** 125121
[91] Zang Y, Ma Y, Peng R, Wang H, Huang B and Dai Y 2021 *Nano Res.* **14** 834
[92] Sun R J, Liu R, Lu J J, Zhao X W, Hu G C, Yuan X B and Ren J F 2022 *Phys. Rev. B* **105** 235416
[93] Whangbo M H, Gordon E E, Xiang H, Koo H J and Lee C 2015 *Acc. Chem. Res.* **48** 3080
[94] Hu H, Tong W Y, Shen Y H and Duan C G 2020 *J. Mater. Chem. C* **8** 8098
[95] Jiang P, Kang L L, Hao H, Zheng X H, Zeng Z and Sanvito S 2020 *Phys. Rev. B* **102** 245417
[96] Lei C G, Xu X L, Zhang T, Huang B B, Dai Y and Ma Y D 2021 *J. Phys. Chem. C* **125** 2802
[97] Zhai B X, Cheng R Q, Yao W, Yin L, Shen C H, Xia C X and He J 2021 *Phys. Rev. B* **103** 214114
[98] Belianinov A, He Q, Dziaugys A, *et al.* 2015 *Nano Lett.* **15** 3808
[99] Ding W, Zhu J, Wang Z, Gao Y, Xiao D, Gu Y, Zhang Z and Zhu W 2017 *Nat. Commun.* **8** 14956
[100] Xiao C, Wang F, Yang S A, Lu Y, Feng Y and Zhang S 2018 *Adv. Funct. Mater.* **28** 1707383
[101] Wu M 2021 *ACS Nano* **15** 9229
[102] Lei C, Li X, Ma Y and Qian Z 2023 *Phys. Rev. B* **108** 155431
[103] Zheng J D, Zhao Y F, Tan Y F, Guan Z, Zhong N, Yue F Y, Xiang P H and Duan C G 2022 *J. Appl. Phys.* **132** 120902
[104] Zhou J, Sun Q and Jena P 2017 *Phys. Rev. Lett.* **119** 046403
[105] Li Y, Liu Y, Wang C, Wang J, Xu Y and Duan W 2018 *Phys. Rev. B* **98** 201407
[106] Liu L, Zhao B, Zhang J, Bao H, Huan H, Xue Y, Li Y and Yang Z 2021 *Phys. Rev. B* **104** 245414
[107] Barik R K and Singh A K 2021 *Chem. Mater.* **33** 6311
[108] Zhan F, Zheng B, Xiao X, Fan J, Wu X and Wang R 2022 *Phys. Rev. B* **105** 035131
[109] Zhan F, Ning Z, Gan L, Zheng B, Fan J and Wang R 2022 *Phys. Rev. B* **105** L081115
[110] Feng X, Xu X, He Z, Peng R, Dai Y, Huang B and Ma Y 2021 *Phys. Rev. B* **104** 075421
[111] Li J, Yao Q, Wu L, Hu Z, Gao B, Wan X and Liu Q 2022 *Nat. Commun.* **13** 919
[112] Chen H, Liu R, Lu J, Zhao X, Hu G, Ren J and Yuan X 2022 *J. Phys. Chem. Lett.* **13** 10297
[113] Pamuk B, Mauri F and Calandra M 2017 *Phys. Rev. B* **96** 024518
[114] Liu J, Li X B, Wang D, Liu H, Peng P and Liu L M 2014 *J. Mater. Chem. A* **2** 6755
[115] Osanloo M R, Saadat A, Van de Put M L, Laturia A and Vandenberghe W G 2022 *Nanoscale* **14** 157
[116] Sun R J, Liu R, Lu J J, Zhao X W, Hu G C, Ren J F and Yuan X B 2023 *Appl. Phys. Lett.* **122** 022404
[117] Huan H, Xue Y, Zhao B, Gao G, Bao H and Yang Z 2021 *Phys. Rev. B* **104** 165427
[118] Cui Q, Zhu Y, Liang J, Cui P and Yang H 2021 *Phys. Rev. B* **103** 085421
[119] Naguib M, Mochalin V N, Barsoum M W and Gogotsi Y 2014 *Adv. Mater.* **26** 992
[120] Wei Y, Zhang P, Soomro R A, Zhu Q and Xu B 2021 *Adv. Mater.* **33** 2103148
[121] Naguib M, Barsoum M W and Gogotsi Y 2021 *Adv. Mater.* **33** 2103393
[122] Zhou C, Zhao X, Xiong Y, Tang Y, Ma X, Tao Q, Sun C and Xu W A 2022 *Eur. Polym. J.* **167** 111063
[123] Dadashi Firouzjaei M, Karimiziarani M, Moradkhani H, Elliott M and Anasori B 2022 *Mater. Today Adv.* **13** 100202
[124] Feng X, He Z, Peng R, Dai Y, Huang B and Ma Y 2022 *Phys. Rev. Mater.* **6** 044001
[125] Lu J J, Liu R, Yue F F, Zhao X W, Hu G C, Yuan X B and Ren J F 2023 *J. Phys. Chem. Lett.* **14** 132
[126] Xu Y, Wang S, Yu S, Wang X, Huang B, Dai Y and Wei W 2022 *J. Phys. Chem. Lett.* **13** 11543
[127] Huang B, Liu W Y, Wu X C, Li S Z, Li H, Yang Z and Zhang W B 2023 *Phys. Rev. B* **107** 045423
[128] Wu Y, Tong J, Deng L, Luo F, Tian F, Qin G and Zhang X 2023 *Acta Mater.* **246** 118731
[129] Jia K, Dong X J, Li S S, Ji W X and Zhang C W 2023 *Nanoscale* **15** 8395
[130] Ma Y, Wu Y, Tong J, Deng L, Yin X, Zhou L, Han X, Tian F and Zhang X 2023 *Nanoscale* **15** 8278
[131] Tong W Y and Duan C G 2017 *NPJ Quantum Mater.* **2** 47
[132] Liu X, Pyatakov A P and Ren W 2020 *Phys. Rev. Lett.* **125** 247601
[133] Zhang T, Xu X, Huang B, Dai Y and Ma Y 2022 *NPJ Comput Mater.* **8** 64
[134] Wu Y, Tong J, Deng L, Luo F, Tian F, Qin G and Zhang X 2023 *Nano Lett.* **23** 6226
[135] Li C L, Wang N B, Hu G C, Yuan X B, Ren J F and Zhao X W 2023 *J. Phys. D: Appl. Phys.* **56** 135301
[136] Li C, Chen H, Hu G, Yuan X, Ren J and Zhao X 2023 *Appl. Phys. Lett.* **123** 243101